ILASS 2008
Sep. 8-10, 2008, Como Lake, Italy

Paper ID ILASS08-2-9

# LARGE EDDY SIMULATION OF AN EVAPORATING SPRAY BASED ON AN EULERIAN-LAGRANGIAN APPROACH

Frederik Hahn*, Clemens Olbricht, Johannes Janicka

University of Technology, Mechanical Engineering, Institute for Energy and Powerplant Technology
Petersenstr. 30, Darmstadt, 64287, Germany
Phone: +49 6151 164103, Fax: : +49 6151 166555
* hahn@ekt.tu-darmstadt.de

## ABSTRACT

Large eddy simulation is assessed concerning the prediction of multi phase flows. Aiming on liquid fuel combustion, characterized by dilute sprays of droplets with relatively small droplets (10-60 μm), an Euler – Lagrangian approach is utilized. Extending previous work, the Lagragnian tracking algorithm is extended with a uniform temperature model to cover droplet evaporation. Both solvers (low-Ma based, geometry flexible, structured, parallelized, sharing memory and search free) are two way coupled. An experimentally well documented evaporating, but non-reacting isopropyl spray is numerically investigated. A comprehensive dataset containing statistical data for both continuous and dispersed phase is provided. Necessary future steps to further assess the prediction quality (e.g. fuel vapor distribution) are raised.

## INTRODUCTION

Combustion is essential for the generation of mechanical energy. As today's civilization is dependent on energy, combustion will be important in future. A variety of reasons (from profitability or efficiency to more restrictive demands of pollutant emissions) call for technological progress in the development of combustion devices. This progress goes hand in hand with deeper understanding of ongoing physics and increased accuracy predicting design modifications. Thus importance of numerical simulations within the design process increases. While for stationary needs gaseous fuels are applicable, especially for mobile devices combustion of liquid fuels is an issue. Within liquid fuel combustion a variety of physical phenomena become important, supplementary to those known from single phase combustion systems. For instance turbulence modulation, two phase mixing, phase transition and chemical reaction, which are all of strongly time dependent nature. While today Reynolds Averaged Numerical Simulation (RANS) is well established in industrial environment, accuracy and predictability suffer from the extensive modelling, neglecting time dependent phenomena, e.g. unsteadiness of turbulence. Large Eddy Simulation (LES), that is well known for its accuracy and potential for predictability concerning one phase flows, modelling only the smaller scales, is valuable to be extended with additional necessary models to achieve predictability for reacting multiphase flows, too. Supremacy of LES versus RANS predicting diffusion flames is strongly based on the improved prediction of mixing processes. Here scalar transport based on large scale structures (coherent and turbulent) is resolved. Beside this the effect and sensitivity to variance modeling (temporary variance in RANS / subgrid-scale variance in LES) is strongly reduced within LES due to its temporal resolution.

Shifting the potential, LES offers, from single phase to two phase combustion, aiming on technical liquid fuel driven combustion systems, several aspects have to be addressed.

Liquid fuelled combustion devices typically are dominated (in terms of fractions of the overall domain) by regions of relatively dilute spray, respectively one phase flow close or behind the flame. Only in regions close to the atomizer dense spray occurs. Under these conditions it seems wise to describe the liquid phase by a Lagrangian approach, contrasting to an ensemble average based Eulerian description. Doing so, an accurate and efficient particle tracking module is indispensable for LES. Unlike RANS within LES summarizing of particles of similar characteristics (position, velocity, diameter, etc.) to representative parcels is inappropriate within most regions of the domain. Only if the particle density within each individual grid cell is high enough at every instant in time physically and statistically assured parcels can be formed. As this can not be safely assumed a priori individual physical particles have to be tracked typically within combustion LES, attaching importance to the efficiency of the Lagrangian tracking.

Combustion heavily depends on the disposition and formation of the gaseous fuel. Thus, beyond dispersion of the liquid fuel droplets, phase transition, precisely evaporation is of major importance for spray combustion. After atomization, including secondary spray break-up, resulting spray droplets normally are in the range of 10-60 μm. These small droplets evaporate while being dragged along by the carrier gas phase. Evaporation takes place mainly based on heat transfer and surrounding fuel vapor pressure. Hence beside evaporation atomization may influence the properties of spray flames.

Improving predictability and accuracy is often based on the knowledge of the most promising fragments, or backwards knowledge of the significant shortcomings. Due to the enormous complexity of multiphase combustion processes evaluation of existing models, combined with LES (if conceptually appropriate) should be done stepwise.

An accurate and efficient particle tracking module combined with LES and it's capabilities under consideration of two way coupling have been shown recently for the case of a non-evaporating particle laden swirl flow, Hahn et al. [1].

In the present paper the performance of a classic equilibrium based uniform temperature evaporation model is investigated. Therefore the validated (dispersion of glass beads) Euler Lagrangian LES solver FASTEST-ECL is extended by an evaporation model.

The investigated configuration is an evaporating isopropyl alcohol spray. This configuration has been studied experimentally by Sommerfeld and Qiu [2]. Distinctiveness of this configuration is that close to the hollow cone pressure atomizer detailed experimental data of the spray characteristics exists, including velocity size correlations for several radii. Based on this data the configuration offers outstanding ability to separate evaluation of evaporation models from atomization modelling. The configuration has been investigated before in the context of LES [3, 4]. In both studies several configurations are investigated aiming on the potential of spray combustion LES, in absence of a detailed discussion of achieved results for this particular case.

In the present study careful an accuracy evaluation of a uniform temperature model is made under the conditions similar to gas turbine sprays. In the following section a brief description of the governing equations and used models is given. Then, the experimental and numerical setup is described. Before concluding the paper a detailed discussion of the achieved results and precision is provided. Therefore continuous and dispersed phase statistics are shown in comparison with experimental data.

## GOVERNING EQUATIONS

Dealing with multiphase flows one typically has two or more sets of conservation equations. In the case of dispersed two phase flows as our case is one gets a set of Eulerian type continuous transport equations and a second set of Lagrangian differential equations describing the actual state of each individual dispersed element.

### Continuous phase

For the continuous phase the conservation equations in the case of low *Ma*-Number flows read as follows. Instantaneous conservation of mass, momentum and conservative scalars are given by

$$\frac{\partial \rho}{\partial t}+\frac{\partial}{\partial x_i}\left(\rho u_i\right)=0, \tag{1}$$

$$\begin{aligned}\frac{\partial}{\partial t}\left(\rho u_i\right) &= -\frac{\partial}{\partial x_j}\left(\rho u_i u_j\right)\\ &+\frac{\partial}{\partial x_j}\left[\mu\left(\frac{\partial u_j}{\partial x_i}+\frac{\partial u_i}{\partial x_j}-\frac{2}{3}\frac{\partial u_k}{\partial x_k}\delta_{ij}\right)\right]\\ &-\frac{\partial p}{\partial x_i}+\rho f_i,\end{aligned} \tag{2}$$

and

$$\frac{\partial}{\partial t}\left(\rho\phi\right)=-\frac{\partial}{\partial x_j}\left(\rho u_j\phi\right)+\frac{\partial}{\partial x_j}\left(\rho D_\phi\frac{\partial \phi}{\partial x_j}\right). \tag{3}$$

Within combustion LES typically at least one additional scalar is transported, here the mixture fraction describing the fuel / oxidizer composition.

Applying the LES filtering formalism to the Eq. (1), (2), and (3) within a hypothetical volume in which multiple phases coexist so that

$$V_{total}(x_i,t)=V_{fl}(x_i,t)+\sum_{prt}V_{prt}(x_i,t) \tag{4}$$

one gets the set of instantaneous conservations equations, characterizing the large scales of the continous phase in dispersed multi fluid systems. The extensive transformation using Leipnitz theorem and Gauss' theorem was first shown by Oefelein [5]. Equation (4) is equivalent to

$$\theta(x_i,t)+\sum_{prt}\theta_{prt}(x_i,t)=1, \tag{5}$$

with

$$\theta=\frac{V_{fl}}{V_{total}},\theta_{prt}=\frac{V_{prt}}{V_{total}}.$$

Here $\theta$ and $\theta_{prt}$ denote the volume fraction and the void fraction, respectively. Making use of this definition for example the equation of mass conservation reads as

$$\begin{aligned}&\frac{\partial}{\partial t}\left(\theta\overline{\rho}\right)+\frac{\partial}{\partial x_i}\left(\theta\overline{\rho}\tilde{u}_i\right)=\\ &\int_{-\infty}^{t}\sum_{prt}\oint_{S(\tau)}\oint\mathcal{H}(x_i-x_{i'},t-\tau)\rho(u_i-w_{i,s})\cdot n_{i,prt}\,dS\,d\tau\end{aligned} \tag{6}$$

The right hand side of the previous equation represents the influence of the dispersed phase. Herein *H* represents the filter kernel, $w_{i,s}$ is the local interface surface velocity, $n_{i,prt}$ is the unit normal face vector, pointing outward from $V_{prt}$. Making use of the thin film assumption, thus one assumes there is no accumulation for example of mass at the interface, jump relations can be defined for mass, momentum and species transport over the interface. Assuming that the volume is small compared to the filter size, meaning that the filter remains constant one gets:

$$\begin{aligned}&\frac{\partial}{\partial t}\left(\theta\overline{\rho}\right)+\frac{\partial}{\partial x_i}\left(\theta\overline{\rho}\tilde{u}_i\right)=\\ &\int_{-\infty}^{t}\sum_{prt}\mathcal{H}(x_i-x_{i'},t-\tau)\left(-\frac{dm_{prt}}{d\tau}\right)d\tau\end{aligned} \tag{7}$$

Please note that *H* is not dimensionless. For example assuming the filter to be a top-hat in all directions, the filter reads:

$$\mathcal{H}(x_j,t)=\begin{cases}\dfrac{1}{\Delta_t}\displaystyle\prod_{j=1}^{3}\frac{1}{\Delta_j} & \text{for} \quad |t|\le\frac{\Delta_t}{2};|x_j|\le\frac{\Delta_j}{2}\\ 0 & \text{else}\end{cases} \tag{8}$$

and for every filter applies

$$\int_{-\infty}^{\infty}\int\int\int_{-\infty}^{-\infty}\mathcal{H}(x_j,t)\,dx_j\,dt=1. \tag{9}$$

Since in implicit LES the grid is supposed to be the filter, often for clearness imagined as a kind of a top-hat filter, the choice of *H* remains open.

Likewise done as for Eq. (1) this procedure can be applied to Eq. (2), and (3) yields for the momentum equations,

$$\begin{aligned}
&\frac{\partial}{\partial t}\left(\theta\bar{\rho}\,\tilde{u}_i\right)=-\frac{\partial}{\partial x_j}\left(\theta\bar{\rho}\,\tilde{u}_i\tilde{u}_j\right)-\frac{\partial\tilde{p}}{\partial x_i}+\bar{\rho}\,g_i\\
&+\frac{\partial}{\partial x_j}\left[\theta\left(\mu\left(\frac{\partial\tilde{u}_j}{\partial x_i}+\frac{\partial\tilde{u}_i}{\partial x_j}-\frac{2}{3}\frac{\partial\tilde{u}_k}{\partial x_k}\delta_{ij}\right)+\bar{\rho}\,T_{ij}^{sgs}\right)\right]\\
&+\int_{-\infty}^{t}\sum_{prt}\mathcal{H}(x_i-x_{i,prt},t-\tau)\\
&-\left(m_{prt}\left(\frac{du_{prt}}{d\tau}-g_i\right)+\frac{dm_{prt}}{d\tau}u_{prt}\right)d\tau,
\end{aligned} \tag{10}$$

and for scalar equations (here mixture fraction),

$$\begin{aligned}
&\frac{\partial}{\partial t}\left(\theta\bar{\rho}\,\tilde{\phi}\right)=\\
&-\frac{\partial}{\partial x_j}\left(\theta\bar{\rho}\,\tilde{u}_j\tilde{\phi}\right)+\frac{\partial}{\partial x_j}\left(\theta\bar{\rho}D_\phi\frac{\partial\tilde{\phi}}{\partial x_j}+\theta\bar{\rho}\,J_j^{sgs}\right)\\
&+\int_{-\infty}^{t}\sum_{prt}\mathcal{H}(x_i-x_{i,prt},t-\tau)\left(-\frac{dm_{prt}}{d\tau}\right)d\tau.
\end{aligned} \tag{11}$$

In Eq. (10) and (11) the terms $T_{ij}^{sgs}$ , and $J_j^{sgs}$ represent the subgrid contribution to the resolved scales. These terms have to be modelled. Physically appropriate models should include aside of single phase flow aspects the effect of dispersed phase / turbulence interaction at the sub-filter scale level. However, since these highly sophisticated models ad a lot of additional complexity we limit us to Smagorinsky type models [6, 7], which are based on an eddy-viscosity ansatz.

**Dispersed phase**

The particle motion is described, as mentioned before, in a Lagrangian framework. Thus based on Newton's 2*nd* law, the equations relevant for particle dynamics are given by

$$\frac{dx_{i,prt}}{dt}=u_{i,prt}, \tag{12}$$

$$m_{prt}\frac{du_{i,prt}}{dt}=\sum_n F_{i,n}. \tag{13}$$

Herein the right hand side of Eq. (13) characterizes all acting forces. In our case, based on the assumptions that the density ratio $\rho_{fl}/\rho_{prt}$ is much smaller than 1, droplets are smaller than the grid-size, that the moment of inertia of particles is negligible, and that of collisions between dispersed particles is negligible, the acting forces reduce to

$$\begin{aligned}
&\frac{1}{m_{prt}}\sum_n F_{i,n}=\\
&\frac{3\,c_w}{4\,D_{prt}}\frac{\rho}{\rho_{prt}}\sqrt{\left(u_j-u_{j,prt}\right)^2}\left(u_i-u_{i,prt}\right)+g_i.
\end{aligned} \tag{14}$$

In Eq. (14) the first term on the right hand side accounts for the effect of the drag force between fluid and dispersed phase. The second term characterizes motion due to gravity. The drag coefficient is evaluated using the correlation given in the following equation,

$$\begin{aligned}
&c_w=\frac{24}{Re_{prt}}\frac{1+.0545\,Re_{prt}+.1Re_{prt}^{.5}\left(1-0.3\,Re_{prt}\right)}{1+a\left|Re_{blow}\right|^b}.\\
&a=0.09+0.077\,e^{-0.4\,Re_{prt}}\\
&b=0.4+0.77e^{-0.04\,Re_{prt}}
\end{aligned} \tag{15}$$

Proposed by Bellan and Harstadt [?]. The above correlation depends on the particle Reynolds number ($Re_{prt}$) and a Reynolds number based on the blowing velocity ($Re_{blow}$),

$$Re_{prt}=\frac{\rho\,L_{prt}}{\mu}\sqrt{\left(u_j-u_{j,prt}\right)^2}, \tag{16}$$

$$Re_{blow}=\frac{\rho\,L_{prt}}{\mu}\left(-\frac{\frac{d}{dt}m_{prt}}{\pi\rho_G D^2}\right). \tag{17}$$

The Lagrangian equations describing the droplet temperature, respectively the droplet mass read,

$$\frac{dT_{prt}}{dt}=\frac{Nu}{3\,Pr_G}\frac{c_{p,G}/c_{p,L}}{\tau_d}\left(T_G-T_d\right)+\frac{L_v}{c_{p,L}} \tag{18}$$

and

$$\frac{dm_{prt}}{dt}=-\frac{Sh}{3Sc_G}\frac{m_{prt}}{\tau_{prt}}\left(T_G-T_{prt}\right)+\frac{L_v}{c_{p,L}}. \tag{19}$$

The characteristic particle time for Stokes flow is defined as

$$\tau_{prt}=\rho_{prt}\frac{D_{prt}^{\ 2}}{18\mu_G}. \tag{20}$$

For Nusselt and Sherwood numbers empirical correlations proposed by Ranz and Marshall [9, 10] accounting for convection effects have been utilized.

### Subgrid-scale effects

With the given sets of Eq. (7)-(11), (12)-(14) and (18)-(19) phase interaction is described for the resolved scales. As considered before, the effect of the particles on the sgs-stress tensor is neglected. Vice versa the effect of the sgs connected phase velocity distribution on the dispersed phase is disregarded. Going to include this effect one has not only to model the unknown velocity distribution, additionally further more restrictive assumptions concerning the particle size have to be made. Going over to spray combustion the sgs-distribution of the mixture fraction becomes important due to the non-linearity of the relation of density and mixture fraction. Common single phase variance modelling based LES approaches are unable to account for the effect of evaporating droplets at sgs-level.

## EXPERIMENTAL AND NUMERICAL SETUP

### Test facility

Sommerfeld and Qiu [2, 11] provided detailed experiments of evaporating sprays. Moderate gas temperatures of the preheated carrier gas phase prevent self ignition. As highlighted before the experiments are outstanding due to the inclusion of the inlet conditions of the spray after secondary breakup. Liquid isopropyl issues via a pressure atomizer into a pre-heated air stream. A sketch of the test section is shown in Figure 1. An annular gap flow enters at the level of the pipe expansion the test section. Co-axial to the gap a hollow cone pressure atomizer is mounted. Sommerfeld and Qiu performed detailed one-component PDA measurements at several downstream locations of the test section. Measurements of all three velocity components were achieved remounting the PDA receiver. Statistical data of gas phase velocities, droplet velocities, droplet sizes and liquid phase mass flux are available. Gas (carrier) phase velocities are only available for the un-laden case due to experimental limitations. Statistical data is available at 7 measurement planes normal to the symmetry axis ranging from 3mm to 400mm downstream the pressure atomizer. Beyond inflow temperature of both phases' wall temperature measurements along the test section are available.

The setup is characterized by well defined boundary conditions for both phases. For the liquid phase particle size versus velocity correlations exist close to the nozzle at 8 different radii, [11].

Flow conditions of the investigated case are listed in Table 1. The rig is set up vertically with gravity acting in downstream direction. This configuration allows to investigate evaporation independent of spray break-up and flame interaction.

### Numerics

All the governing equations have been implemented into the three dimensional CFD code FASTEST-ECL. The code uses geometry-flexible, block-structured, boundary fitted grids. This enables FASTEST-ECL to represent complex geometries like the investigated ones. A collocated grid with a cell-centered variable arrangement is used. The flow solver offers fully second order accuracy. Discretization is based on the finite volume method. For spatial discretization specialized central-differencing schemes are utilized, see Lehnhäuser and Schäfer [12]. To assure boundedness of the mixture fraction, the convective term in the scalar transport Eq. (11) has been discretized using non oscillatory bounded TVD schemes [13]. For the time stepping multiple stage Runge-Kutta schemes (here: three stages) with second order accuracy are utilized.

Following a fractional step formulation, in each stage a momentum correction is carried out in order to satisfy the continuity. Therefore a Poisson equation is derived from Eq. (1) and solved iteratively with multi-grid and SOR relaxation. The Lagrangian particle tracking algorithm is second order accurate in space consistent to the flow solver. It is search free, taking advantage of the block structured grids, resulting in a high efficiency. The equations of particle motion and state are solved with an adaptive $5^{th}$ order accurate multi step Runge-Kutta method.

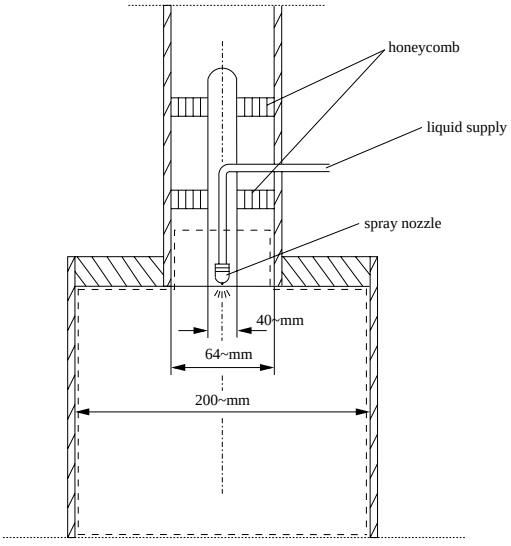


Fig. 1: Experimental test facility.

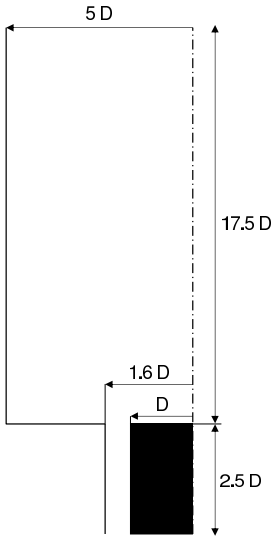


Fig. 2: Computational domain.

Table 1: Flow conditions.

| Case | Air volume flow [$m^3/s$] | Air mass flow [g/s] | Maximum air velocity [m/s] | Maximum air temperature [°C] | Liquid mass flow rate [g/s] | Liquid inlet temperature [°C] |
|---|---|---|---|---|---|---|
| Unladen flow | 0.032 | 29.0 | 18.0 | 100 | - | - |
| Laden flow | 0.031 | 28.3 | 18.0 | 100 | 0.44 | 34 |

The phase interaction source terms in Eq. (7), (10)-(11) are modelled to be evaporated/condensed mass and drag forces summarized over all particles in one grid cell.

To ensure an accurate and efficient coupling of the solvers of both phases the $5^{th}$ order Runge-Kutta scheme of the Lagrangian solver is embedded into the $3^{rd}$ order Runge-Kutta scheme of the Eulerian flow solver, justified under consideration of the scale separation of both problems.

FASTEST-ECL is parallelized by domain decomposition using the MPI message passing library.

A sketch of the computational domain is shown in Fig. 2. The domain is discretized using 3d O-grid technique, obtaining an increased spatial resolution in the region near the pressure atomizer and in the inlet duct. This yields a grid with a total of $1.8 \cdot 10^6$ cells. Elliptical smoothing has been applied to improve grid quality.

Parallelization via domain decomposition was made under consideration of adequate load balancing between all CPUs for both solvers.

At the outlet convective outlet boundary conditions were used for the plane normal velocity component where as for orthogonal velocities zero gradient boundary conditions are chosen. Naturally no slip boundary conditions are used at the walls. For the inlet mean velocities are superposed with turbulent fluctuations. These fluctuations are generated using the digital filters method, [14].

Droplets are injected/initialized in a plane 3mm downstream of the pressure atomizer. Based on measured mass fluxes each individual physical particle is injected. Droplet position, velocity and sizes are with different random processes at eight coaxial radial rings of 1mm thickness, forming together a circle of 8mm radius. While the droplets are uniformly distributed along the circles, droplet velocities and diameters are based on measured mean and variance assuming a Gaussian probability distribution. The number of injected droplets depends of the measured mass flow, left over droplet fractions are injected at the next time step. If the droplet diameter becomes lower the 1µm, the droplet is to evaporate at once, fully conserving mass and momentum. In Fig. 8 the evolution of the number of droplets inside of the domain is shown. After 1.5 flow through times (based on maximum inflow velocity) a quasi steady state is achieved giving approximately $260 \cdot 10^3$ droplets inside of the domain. In seldom cases if droplets reach the walls droplets are reflected fully conserving of their kinetic energy.

Single phase statistics cover a range of 7 flow through times. Multi phase statistics are started 3 flow through times after begin of droplet injection, and samples are collected for 25 flow through times.

## RESULTS

In Figure 3 a snapshot of the instantaneous axial carrier phase velocity in a plane cutting the symmetry axis is shown. The snapshot reveals the highly instationary nature of this flow and gives qualitatively an impression of the smallness of the resolved structures. The large potential of LES predicting dispersed flows becomes apparent, resolving significantly more than integral scales. These are the ones being inherently meaningful for the evolution of each droplet.

As an accurate prediction of the carrier phase is indispensable for two phase flow prediction statistical results for the unladen case are examined first. In Figure 5 gas phase velocity statistics are compared with available experimental data of the unladen case. Generally very good agreement between experiment and simulation can be observed. Starting at the first measurement plane downstream the unused spray nozzle very good agreement for mean axial velocity is found. The level of axial velocity fluctuation is reproduced accurately. Only the peak values of the fluctuations inside the inner and outer shear layers of the gap-flow are under predicted, nevertheless qualitatively reproduced. For the radial velocity the simulation already shows some constriction while the experiment does not. However the radial velocity is very small compared to axial velocity, probably the plane were constriction takes effect is misspredicted. In the second plane agreement between experiment and simulation improves. The plot of the mean axial velocity reveals a slight of axis deviation of the experiments, that is confirmed in downstream planes.

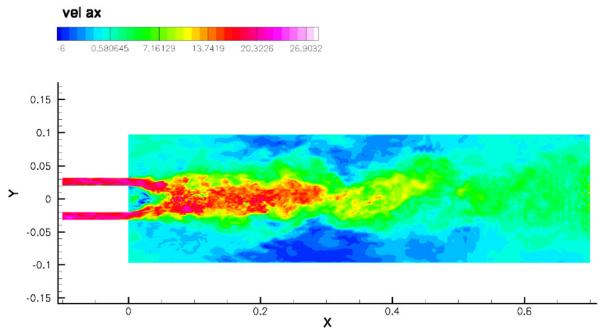


Fig. 3: Impression of the unsteady carrier phase velocity field.

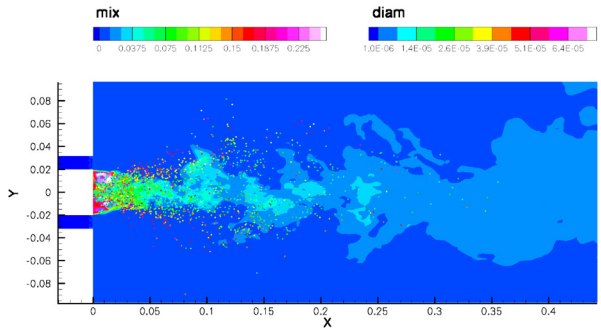


Fig. 4: Impression of the unsteady droplet distribution.

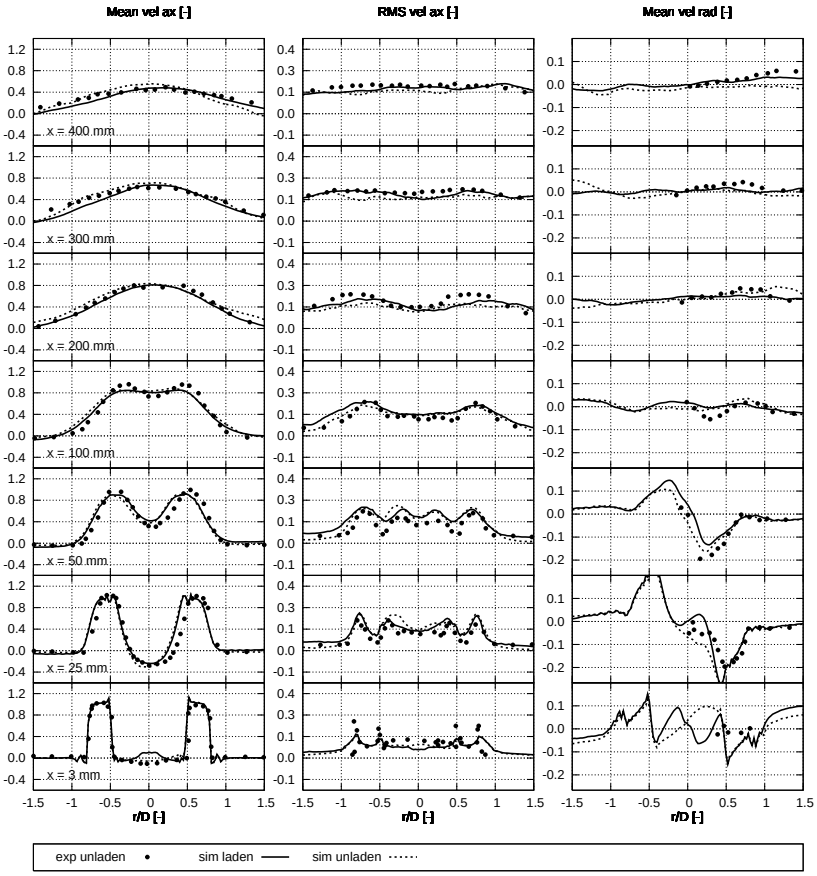


Fig. 5: Continuous phase velocity statistics.

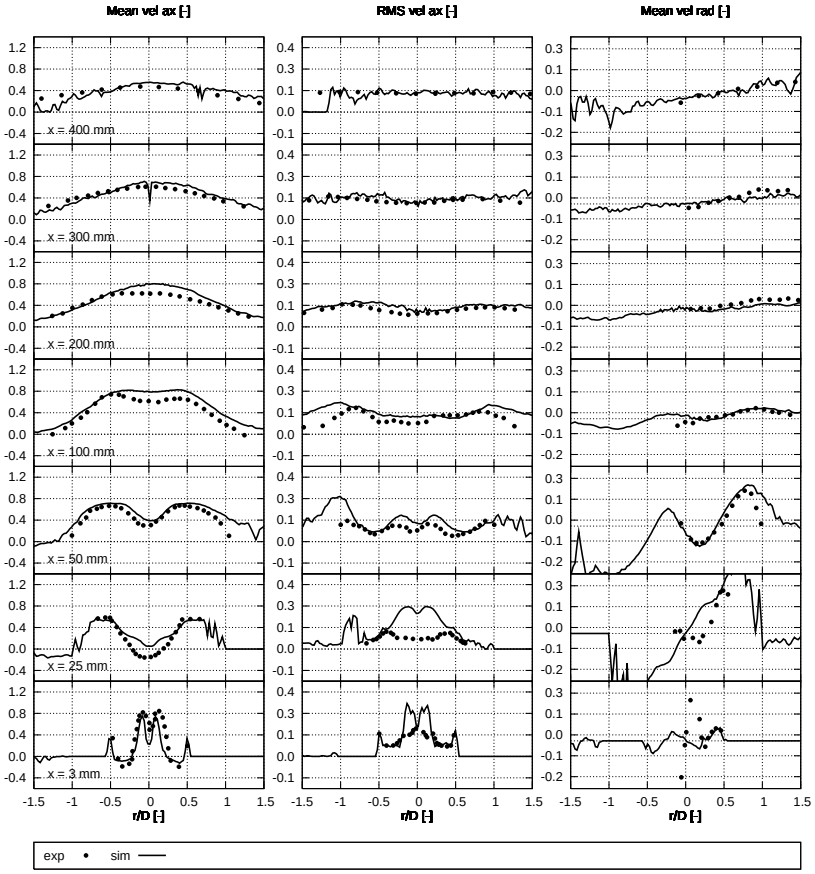


Fig. 6: Dispersed phase velocity statistics.

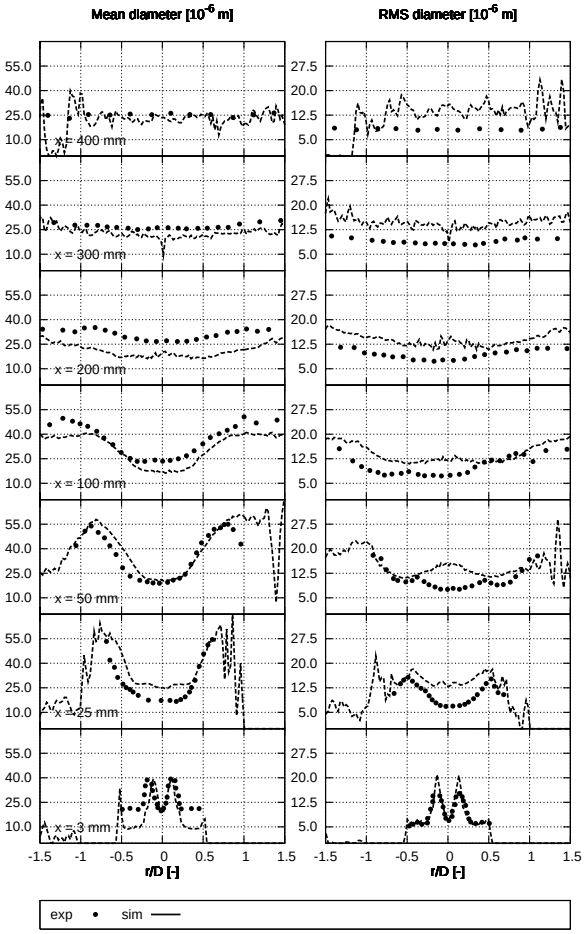


Fig. 7: Droplet diameter statistics.

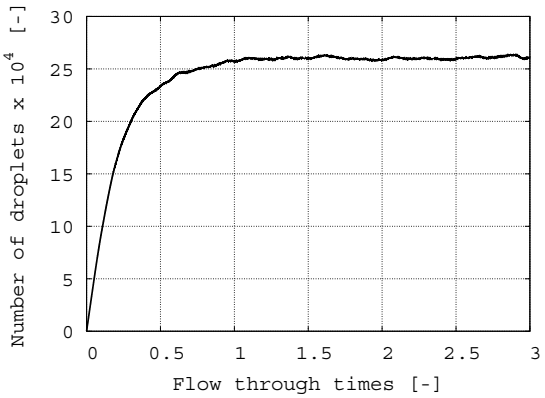


Fig. 8: Accumulation of droplets inside of the numerical domain after of droplet injection begins.

Considering this, level and shape of mean and variance of the axial velocity are nicely captured. For the mean radial velocity the simulation gives good results in terms of level and shape. The same observations can be drawn from the next plane 50mm downstream the nozzle. In the next plane (100mm) first effects of an over predicted diffusivity can be noticed. The simulation mean axial velocity profile has slightly broadened compared to the experiments. Furthermore the incision in the profile around the symmetry axis has been smeared out. While axial velocity fluctuations are still predicted very good, the radial velocity profile shows very good agreement only away from the symmetry axis, coinciding to the findings for the mean axial velocity. None the less the quality of the prediction of the radial velocity is still impressive. For the next three planes, located 200mm, 300mm and 400mm downstream the nozzle quality of the predictions is excellent. Minimal deviations can be found for the radial velocity. The order of these is negligible and may be related to statistical uncertainties. In Figure 5 the gas phase velocities for the droplet laden case are shown, also. Two things have to be mentioned. First, the gas phase velocity is only significantly influenced close to the spray nozzle where relatively dense spray occurs. Second, it seems that the extended simulation time lead to noticeable improved statistical convergence.

Going over to the dispersed phase in Fig. 4 a instantaneous snapshot of the evaporating droplets is shown. Droplets in a sheet of 0.5mm thickness intersecting the symmetry axis are presented coloured by their diameters. In the background a plane of the corresponding momentary present mixture fraction distribution is depicted. The decreasing droplet density downstream is obvious. In Figure 6 profiles of the dispersed phase velocities are shown. Numerical results are presented together with experimental data. The first measurement plane coincides with the plane where droplets have been initialized. While the mean axial velocity shows good agreement between simulation and measurements, axial velocity fluctuations and radial mean velocity both reveal initialization problems in the core region of the spray. Outside of the core region axial fluctuations and radial velocity show good agreement. Inside the fluctuations are over predicted while radial movement is under predicted. A possible explanation is that the recirculation zone has strong influences, due to an overlay of injected droplets with recirculated ones. For the second plane the simulation fails to predict the inner recirculation zone. Outside of the recirculation zone good agreement between experiment and simulation is obtained. Again axial fluctuations are over predicted in the core region, where recirculation should occur. Radial velocities are reproduced only qualitatively. In regions where experimentally no data has been recorded the simulation statistics show large variations, indicating insufficient samples. In the next plane 50mm downstream the nozzle very good agreement between simulation and measurements is obtained. For mean axial velocity, its variance and mean radial velocity characteristic features are reproduced, levels match precisely. In the next plane agreement is very good again. Consistently to the carrier phase statistics the mean axial velocity profile is broadened and slightly smoothened. The level of axial velocity fluctuations is nicely reproduced. Results for mean radial velocity impressively match the experimental results. The next three planes downstream (200mm, 300mm and 400mm) show similar level of accuracy. Due to the fact that the majority of droplets is already evaporated the statistical error increases, leading to wiggling of the lines. The potential of two phase LES predicting dispersed phase velocity is obvious. Summarizing the dispersed phase velocity statistics it seems to be most problematic to carry out a proper initialization of the dispersed phase. This of course is strongly linked to a proper modelling of the atomization process.

The evaluation of the accuracy of the evaporation model can be done by comparison of droplet diameter statistics. In Figure 7 droplet statistics are shown. Again simulation results are compared with experimental data. Here the mean diameter and its variance are shown. In the first plane where droplets are initialized good agreement can be found as expected. In

the second plane both diameter and its variance are qualitatively reproduced. While the diameter is slightly over predicted its variance is considerably over predicted in the core region. This corresponds to previous findings, again problems with the recirculation of droplets may be the reason. For the third plane (50mm) the mean droplet diameter is accurately predicted. Taking a detailed look one detects a slight off-axis shift of the experiments. This unphysical shift is the cause for minor discrepancies. The asymmetry of the simulation results in the outer regions is linked to insufficient statistics. Prediction quality of the droplet diameter variances is ambivalent. In the outer region level and shape reproduce measurements, while close to the symmetry axis the shape is different and the fluctuations level is 50% over predicted. For the next two planes (100mm and 200mm) the droplet diameter is under predicted while the fluctuations are over estimated. Under prediction of the diameter may be a result of the utilization of the uniform temperature model. This model is known to give an under estimate of the evaporation time for small droplets and / or high evaporation rates, [15]. For the last two measurement planes (300mm and 400mm) the estimated and the measured droplet diameter show better agreement again. Notably statistical errors increase going downstream. This is a result of the reduced droplet mass flux, as most droplets are already evaporated. For both planes droplet diameter fluctuation is over predicted. In general, keeping in mind the simplicity of the approach, impressive results have been obtained. Especially the dispersed phase statistics are promising. Quality of the velocity statistics is in line with results of previous non-evaporating dispersed configurations as expected. Considering the complexity of physical phenomena taking place in evaporating two flows, the accuracy of the diameter statistics is remarkable.

## CONCLUSION

A step extending LES, aiming on liquid fuel combustion, has been made. The straight forward approach combining “high fidelity” LES with a Lagrangian two phase formalism rather trying to resolve transient physical phenomena than include sophisticated models showed great potential. Utilization of an efficient low-Mach number assumption based Eulerian solver in combination with an efficient search free Lagrangian tracking algorithm, both taking advantage of block structured geometry flexible grids, allowed tracking of physical existing droplets in a well resolved turbulent field. Within this approach the price to be paid is the limitation to simple, computationally cheap evaporation models. Here a uniform temperature model has been applied. Very good agreement between experimental data and simulation results is obtained for both phases velocities. Furthermore the mean droplet diameter predictions are in good agreement. The analysis of the predicted diameter fluctuations gives good results, respectively shows an overestimation for some regions. As two phase interaction effects on sgs-level have been completely neglected and established models typically enforce fluctuations of the dispersed phase a new strategy to cover this is necessary. Future work should address this. Furthermore aiming at two phase combustion where transient fuel vapor distribution is of major importance ways to assess this quantity have to be developed.

## ACKNOWLEDGMENT

The authors gratefully acknowledge the *Deutsche Forschungsgemeinschaft* for financial support through SFB 568 "Flow and Combustion in Future Gas Turbine Combustion Chambers". All computations have been performed on the Hessian High Performance Computer (*HHLR*), supported by the activity group on High Performance Scientific Computing (*HPSC*), a member of the computational engineering center (*FZCE*) Darmstadt.

## REFERENCES

[1] F. Hahn, A. Sadiki and J. Janicka, Large Eddy Simulation of a Particle Laden Swirling Flow Based on an Eulerian-Lagrangian Approach. *Proc. of the ICMF*, vol. 6, 2007.

[2] M. Sommerfeld and H. H. Qiu. Experimental studies on spray evaporation in turbulent flow. *Int. J. Heat and Fluid Flow*, 19:10–22, 1998.

[3] P. Moin and S.V. Apte, Large Eddy Simulation of Realistic Gas Turbine Combustors, *AIAA J.*, vol. 44, pp. 698-708,2006.

[4] S. James, J. Zhu and M.S. Anand, Large-Eddy Simulations as a Design Tool for Gas Turbine Combustion Systems, *AIAA J.*, vol. 44, pp. 674-686,2006.

[5] J. C. Oefelein. Large eddy simulation of turbulent combustion processes in propulsion and power systems. *Prog. in Aerospace Sciences*, vol. 42,pp. 2-37, 2006.

[6] J. Smagorinsky. General circulation experiments with the primitive equations: I. the basic equations. *Mon. Weather Rev.*, vol. 91, pp. 99-164, 1963.

[7] D. K. Lilly. A proposed modification of the germano subgrid-scale closure method. *Phys. Fluids A*, vol. 4, pp. 633-635, 1992.

[8] J. Bellan and K. Harstadt. The details of evaporation of dense and dilute clusters of drops. *Int. J. Heat Mass Transfer* , vol. 30, pp.125-136, 1987.

[9] W.E. Ranz and W.R. Marshall. Evaporation from drops: I. *Chem. Engng. Prog*., vol. 48, pp. 141-146.

[10] W.E. Ranz and W.R. Marshall. Evaporation from drops: II. *Chem. Engng. Prog*., vol. 48, pp. 173-180.

[11] M. Sommerfeld and H. H. Qiu. Experimental studies on spray evaporation in turbulent flow. *Proc. Of the 7th Workshop on Two Phase Flow Predictions*, 1994.

[12] T. Lehnhauser and M. Schafer. Improved linear interpolation practice for finite-volume schemes on complex grids. *Int. J. Numer. Meth. Fluids*, vol. 38, pp. 625-645, 2002.

[13] Hahn, F., Olbricht, C. and Janicka., J. (2008) Study of various configurations under variable density mixing conditions aiming on gas turbine combustion using LES. *Proc. of the ASME Turbo Expo: Power for Land, Sea and Air*, GT2008-50268, 2008.

[14] M. Klein, A. Sadiki, and J. Janicka. A digital filter based generation of inflow data for spatially developing direct numerical or large eddy simulation. *J. Comput. Physics*, vol. 186, pp. 652-665, 2003.

[15] R.S. Miller, K. Harstadt and J. Bellan. Evaluation of equilibrium and non-equilibrium evaporation models for many-droplet gas-liquid simulations. *Int. J. Multiphase Flow*, vol. 24, pp. 1025-1055, 1998.